Marine Biotechnology
August 2022, Volume 24 Issue 4 Pages 801-819
https://doi.org/10.1007/s10126-022-10150-y
https://archimer.ifremer.fr/doc/00787/89929/

Mechanically Enhanced *Salmo salar* Gelatin by Enzymatic Cross-linking: Premise of a Bioinspired Material for Food Packaging, Cosmetics, and Biomedical Applications

Buscaglia Manon [1], Guérard Fabienne [1], Roquefort Philippe [2], Aubry Thierry [2], Fauchon Marilyne [1], Toueix Yannick [1], Stiger-Pouvreau Valerie [1], Hellio Claire [1], Le Blay Gwenaëlle [1, *]

[1] Univ Brest, CNRS, IRD, Ifremer, LEMAR, F-29280, Plouzané, France
[2] UMR CNRS 6027, IRDL, Université de Bretagne Occidentale, 29200, Brest, France

* Corresponding author : Gwenaëlle Le Blay, email address : gwenaelle.leblay@univ-brest.fr

Abstract :

Marine animal by-products of the food industry are a great source of valuable biomolecules. Skins and bones are rich in collagen, a protein with various applications in food, cosmetic, healthcare, and medical industries in its native form or partially hydrolyzed (gelatin). Salmon gelatin is a candidate of interest due to its high biomass production available through salmon consumption, its biodegradability, and its high biocompatibility. However, its low mechanical and thermal properties can be an obstacle for various applications requiring cohesive material. Thus, gelatin modification by cross-linking is necessary. Enzymatic cross-linking by microbial transglutaminase (MTG) is preferred to chemical cross-linking to avoid the formation of potentially cytotoxic residues. In this work, the potential of salmon skin gelatin was investigated, in a comparative study with porcine gelatin, and an enzymatic versus chemical cross-linking analysis. For this purpose, the two cross-linking methods were applied to produce three-dimensional, porous, and mechanically reinforced hydrogels and sponges with different MTG ratios (2%, 5%, and 10% w/w gelatin). Their biochemical, rheological, and structural properties were characterized, as well as the stability of the material, including the degree of syneresis and the water-binding capacity. The results showed that gelatin enzymatically cross-linked produced material with high cross-linking densities over 70% of free amines. The MTG addition seemed to play a crucial role, as shown by the increase in mechanical and thermal resistances with the production of a cohesive material stable above 40 °C for at least 7 days and comparable to porcine and chemically cross-linked gelatins. Two prototypes were obtained with similar thermal resistances but different microstructures and viscoelastic properties, due to different formation dynamics of the covalent network. Considering these results, the enzymatically cross-linked salmon gelatin is a relevant candidate as a biopolymer for the production of matrix for a wide range of biotechnological applications such as food packaging, cosmetic patch, wound healing dressing, or tissue substitute.

Keywords : Cross-linking, Marine biomaterial, Microbial transglutaminase, Rheology, Salmon gelatin

1. Introduction

Gelatin is a protein obtained from partial hydrolysis of collagen (Lv et al. 2019). Collagen is the most abundant protein in vertebrate organisms, as a primordial extracellular component representing up to 30% of their total proteins (Bae et al. 2008; Berendt et al. 2008; Gu et al. 2019). Its structure is a three-dimensional triple helix combining α-chains connected by hydrogen bonds. The collagen molecules are linked together to form fibers providing flexibility, stability and resistance to tissues (Gelse et al. 2003; Bhagwat and Dandge 2018). The gelatin is formed by free α chains that can arrange themselves in a triple helix, like collagen structure, if the gelling temperature is reached (coil → helix transition) (Harrington and Rao 1970; Djabourov 1988; Bello et al. 2020). Gelatin, as collagen, is a biopolymer used in various industrial fields such as food, cosmetic, healthcare and medical industries (Gómez-Estaca et al. 2009; Huang et al. 2019; Lv et al. 2019). This protein has been attracting the attention of manufacturers and scientists for decades due to its wide range of applications as stabilizer, texturizer, cohesion agent, protein provider, film protector or moisture preserver (Ehrlich 2015; Lv et al. 2019). Gelatin has promising applications in food manufactures as packaging or edible coatings for meat products (Battisti et al. 2017; Díaz-Calderón et al. 2017; Prasad 2021), in healthcare as edible capsules releasing bioactive nutrients or in medicine with recent developments as polymer for wound healing dressing and tissue engineering with the 3D printing (Van Vlierberghe et al. 2011; Acevedo et al. 2019; Echave et al. 2019; Bello et al. 2020; Da Silva et al. 2021; Prasad 2021). This molecule enables the recovery of animal parts intended for animal meal production as it is extracted from by-products of the food industry, such as skin and bones. This recovery is environmentally beneficial with a zero-waste approach but also economically by obtaining high value-added products from discarded biomass (Silvipriya et al. 2015; Huang et al. 2019; Nitsuwat et al. 2021).

Gelatin-based biomaterials are widely used as basic matrices due to their biocompatibility, biodegradability, low antigenicity, cell growth potential and adaptable mechanical properties (Broderick et al. 2005; Van Vlierberghe et al. 2011; Echave et al. 2019; Lv et al. 2019). Generally, used gelatin has mammalian origin, mainly bovine and porcine (Ferraro et al. 2010; Nitsuwat et al. 2021). This origin raises health concerns with the possible transmission of infectious vectors such as prions and may not conform to certain cultural and religious restrictions for some Muslim and Jewish communities (representing almost 23% of world's population) (Charulatha and Rajaram 2003; Song et al. 2006; Karim and Bhat 2009; Huang et al. 2019). To overcome these constraints other gelatin sources with high biocompatibility and similar structural and mechanical properties have to be found.

Marine gelatin from fishing by-products could be an interesting alternative since it represents a huge source of collagen that can provide gelatin. Currently, about 50-75% of the total catch weight represents a waste of raw materials that contains about 30% of skin and bones very rich in collagen (Jongjareonrak et al. 2005; Bode et al. 2011; Bhagwat and Dandge 2018). Marine gelatin is as biocompatible as mammalian gelatin but it is less stable due to a lower content of proline and hydroxyproline, which stabilize the gel structure by creating hydrogen bonds (Jongjareonrak et al. 2006; Gómez-Estaca et al. 2009; Ferraro et al. 2010; Da Silva et al. 2014). This difference results in lower gelling and melting temperatures, but also in poorer physical and rheological properties for marine gelatin biomaterial (Gomez-Guillén et al. 2001; Haug and Draget 2011; Huang et al. 2019). This latter cannot therefore be used in applications requiring a thermal stability and high bloom degree (Karim and Bhat 2009; Ferraro et al. 2010). However, cross-linking reactions can improve these properties by

amplifying the formation of new covalent bonds within the material (Bigi et al. 2001; Song et al. 2006). Stronger network removes the thermoreversible ability of gelatin to change state (Gomez-Guillén et al. 2001). Most commonly, chemical cross-linking agents are used, such as glutaraldehyde (GTA) or carbodiimides, as they are very effective. However, they present risks of cytotoxicity, and produce inflammatory reactions or tissue calcification (Chau et al. 2005; Chen et al. 2005; Barnes et al. 2007; Annamalai et al. 2019), which should be avoided in food, cosmetic or healthcare applications. An alternative method such as enzymatic cross-linking with microbial transglutaminase (MTG, EC.2.3.2.13) is then necessary. This food grade enzyme has a good cytocompatibility and it is recognized as safe for human ingestion (Huang et al. 2019; Adamiak and Sionkowska 2020). MTG catalyzes acyl transfer reactions between γ-carboxyamide groups of peptide-bound glutamine residues (acyl donor) and ε-amino groups of mainly lysine residues (acyl acceptor) that creates intermolecular or intramolecular ε-(γ-glutamyl)lysine bonds (Folk 1970). Mechanical and proteolytic resistances are then increased without creating cytotoxic residues (Stachel et al. 2010; Zhao et al. 2016; Liu et al. 2020).

In this study, the gelatin was obtained from Atlantic salmon (*Salmo salar*) skins. This species was chosen because its annual world production is 2.4 million tons (4.5% of the aquaculture fish production) for the food industry, which allows for sustainability, consistency of quality and traceability of the resource (FAO 2020). The properties of the gelatin were improved with MTG to obtain a biomaterial harboring mechanical and thermal properties adaptable to the different applications. To understand this subject, a deeper knowledge of the protein enzymatic cross-linking phenomena is required by the study of gelling properties. Thus, the objective of this study is to determine the optimal amount of enzyme needed to obtain a biomaterial capable of competing with chemical cross-linking and mammalian gelatin. The developed biomaterial was analyzed as hydrogel (highly hydrated matrix) and sponge (freeze-dried matrix). The efficiency of the cross-linking by MTG was performed with structural, biochemical and mechanical analyses. Attained results could find a practical application in controlling the structure of salmon gelatin with well-defined physical properties adaptable for various applications such as food packaging, cosmetic patch, wound healing dressing or tissue substitute (Morimura et al. 2002; Bhagwat and Dandge 2018; Prasad 2021).

2. Materials and methods

2.1. Material origins

2.1.1. Biological materials

Gelatin from salmon was extracted by YSLAB company (Quimper, France) from skins obtained from MerAlliance company (Quimper, France) according to the patent WO 2016/142633 (Hemon et al. 2016). Salmon skins were cleaned, coarsely ground to increase the extraction yield and washed twice with 0.45M NaCl and clear water. Subsequently, thermal hydrolysis was performed at 45°C for 60 min under stirring followed by successive filtrations down to 0.4 mm. The supernatant containing gelatin was frozen at -20°C and freeze-dried. The resulting dry material was solubilized at 6% (w/v) in distilled water at 40°C and clarified by a 10-min centrifugation at 8000 g at 20°C to remove hydrophobic components (centrifuge 5810 R, Eppendorf, France). The supernatant was collected and freeze-dried for use in the following tests. Type A gelatin from porcine skin (300 bloom, BioReagent, Sigma-Aldrich, USA) extracted by acid procedure was used for comparison in cross-

linking impacts. MTG was donated by BDF ingredients (Girona, Spain) in a powder form. The enzyme was obtained from the bacteria *Streptomyces mobaraensis* and the nominal activity was 125 $U.g^{-1}$ of powder.

2.1.2. Chemical materials

All chemicals and reagents used in this study were analytical grade. Buffer reagents, as sodium dihydrogen phosphate ($NaH_2PO_4 \bullet H_2O$), di-sodium hydrogen phosphate dodecahydrate ($Na_2HPO_4 \bullet 12H_2O$) and sodium chloride (NaCl), were purchased from Carlo Erba Reagents (France). SDS-PAGE assay reagents and materials were received from Bio-Rad Laboratories (USA). Protein molecular weight markers for size-exclusion chromatography (SEC-HPLC), sodium dodecyl sulfate (SDS), sodium azide, albumin from bovine serum (BSA), 2-mercaptoethanol (BME), L-Leucine and *o*-phthalaldehyde (OPA) were obtained from Sigma-Aldrich (USA). GTA (25% aq. solution) was purchased from Alfa Aesar (Germany).

2.2. Material characterization

The proximate analysis of the salmon gelatin were performed by UpScience (Vannes, France). Moisture content was determined gravimetrically by oven drying at 103°C for 4 h *(Internal method EAU-H 14)*. Fat content was obtained by gravimetric method after a hot treatment with hydrochloric acid followed by filtration, extraction with petroleum ether, solvent removal by distillation and residue drying (*Internal method MGRA-H 15 – process B*). Protein content was assessed by Dumas methodology (with a conversion factor of 5.4) (*Internal method DUMAS-H 14*) (Jongjareonrak et al. 2006). Total ash content was determined gravimetrically by a furnace (*Internal method CEND-H 13*).

Salmon and porcine gelatins were characterized by SDS-PAGE according to the method of Laemmli (1970) and the supplier instructions. Briefly, freeze-dried samples were dissolved in distilled water to 1 $g.L^{-1}$ and kept in a water bath at 40°C for 30 min. Solubilized samples were mixed at 1:1 (v/v) ratio with the Laemmli sample buffer (62.5 mM Tris-HCl pH 6.8, 2% SDS, 25% (v/v) glycerol, 0.01% bromophenol blue and 5% (v/v) BME freshly added). The mixtures were denatured in boiled water at 95°C for 5 min. Samples (20 µL) and protein markers (10 µL of Precision Plus Protein Standards Dual Colors) were loaded onto 4-20% polyacrylamide gel (Mini-Protean TGX) and submitted to electrophoresis at 150V using Mini-Protean Tetra System. After electrophoresis, gel was rinsed with distilled water and fixed with a solution of 50% (v/v) methanol and 10% (v/v) acetic acid for 30 min. Then, gel was stained with Bio-Safe Coomassie G-250 Stain overnight and destained with a solution of 10% (v/v) acetic acid for 30 min four times. The profiles of salmon and porcine gelatins were compared using a Gel Doc EZ Imager and the software Image lab 5.0.

Molecular weight distribution and proportion of salmon and porcine gelatins were estimated by SEC-HPLC according to GE Healthcare instructions on a device Dionex Ultimate 300 $UHPLC^+$ focused (ThermoFisher Scientific, France). Samples were suspended at 20 $g.L^{-1}$ in the mobile phase (0.05 M phosphate buffer containing 0.15 M NaCl and 0.02% (w/v) sodium azide, pH 7.2) and heated at 40°C for 30 min before filtration on 0.22 µm Millex PTFE filters (Merck Millipore, Ireland). Samples (10 µL) were loaded on a Superdex 200 10/300 GL column (GE Healthcare, Sweden) previously equilibrated with the mobile phase. The flow rate was 0.5 $mL.min^{-1}$ and all the system was heated at 35°C. Compounds leaving the column were detected at 220 and 280 nm and data were analyzed with Chromeleon 7 (ThermoFisher Scientific, France). The column was calibrated with standard compounds: thyroglobulin (669 kDa), apoferritin (443 kDa), β-amylase (200 kDa),

alcohol dehydrogenase (150 kDa), albumin (66 kDa) and carbonic anhydrase (29 kDa) from Gel filtration markers kit 29-700 kDa (Sigma-Aldrich, USA) and cytochrome c (12.3 kDa) (Sigma-Aldrich, USA). The relation between retention time (RT) and molecular weight (MW) was: log (MW) = -0.113 x RT + 5.0793.

The amino acid compositions of salmon and porcine gelatins were determined by UpScience (Vannes, France) according to an internal method adapted from the EC regulation 152/2009 of January 27, 2009 (Commission 2009). Briefly, samples were hydrolyzed in hydrochloric acid and/or oxidized with performic acid. They were separated on ion exchange chromatography and then characterized by reaction with ninhydrin using photometric detection at 440 and 570 nm. Amino acid contents of samples were reported as g/100g of protein.

2.3. Cross-linking procedures

Freeze-dried salmon and porcine gelatins were hydrated in phosphate buffer 0.1 M (pH 6) containing 0.02% (w/v) sodium azide at 40°C for 30 min, to obtain a complete dissolution. This temperature is optimal for MTG and it partially denatures gelatin network to subsequently improve cross-linking (Stachel et al. 2010). Then, MTG solubilized in phosphate buffer was added, and the mixture was stirred manually until homogenization. At the end, the gelatin was at 6.67% (w/v) (Jongjareonrak et al. 2006; Arnesen and Gildberg 2007; Mohtar et al. 2013) and MTG was tested at three concentrations: 2%, 5% and 10% (w/w gelatin) (representing 2.5, 6.25 and 12.5 $U.g^{-1}$ of gelatin respectively) (Table 1). The mixtures were incubated in a water bath at 40°C for 30 min and the enzyme was inactivated by heating the samples up to 70°C for 15 min (Gomez-Guillén et al. 2001; De Carvalho and Grosso 2004). The hydrogels were left at room temperature for 20 min and then at 4°C for at least 18 h. Samples were used for measurements under hydrogel or sponge forms after a freeze-drying step.

The negative control (called native is the untreated gelatin) was made using the same procedure with phosphate buffer instead of the MTG solution. The positive control was a chemical cross-linking with 1% (v/v) GTA without heating after GTA addition. All the following tests were carried out in triplicate.

2.4. Rheological characterization

Rheological measurements were carried out in oscillatory shear on a MCR 702 MultiDrive rheometer (Anton Paar, France), following a previously proposed procedure (Mohtar et al. 2013). The storage modulus (G'), which characterizes the elastic energy stored in the sample, and the loss modulus (G''), which characterizes the viscous dissipation within the sample, were studied at a constant frequency of 1 Hz and at a strain amplitude of 1%, chosen in the linear regime. All viscoelastic data were analyzed with the software Anton Paar RheoCompass 1.24.

2.4.1. State transitions of native gelatins (sol-gel and gel-sol)

State transitions of native gelatins (S-NAT and P-NAT) were measured in a concentric-cylinder geometry stainless steel and titanium (17 mm diameter bob and cup, inner diameter: 16.65 mm, outer diameter: 18.08 mm, length: 25 mm, gap: 0.71 mm). Approximately 4.6 mL of 5% (w/v) gelatin solution were loaded into the geometry and a thin layer of paraffin oil was applied over the sample and the geometry to prevent drying. Sample was cooled down at a rate of 0.5°C.min^{-1} from 40°C to about 3°C under the sample gelling temperature. Sample was maintained at the lowest temperature for 1 h in order to complete the gelling process. The melting

temperature was obtained by increasing the temperature to 40°C at a rate of 0.5°C.min^{-1}. The gelling point (or the sol-gel transition) and the melting point (or gel-sol transition) were determined as the cross-over points of G' and G'' (Djabourov et al. 1988b).

2.4.2. Cross-linking impact on thermal resistance

Thermal resistances of native and cross-linked gelatins were carried with a sandblasted stainless steel parallel-plate geometry of 25 mm diameter. Hydrogels were prepared as previously described in Petri dishes in a layer of 1 mm thick and left at 4°C for at least 18 h. A piece of hydrogel was removed with a punch of 25 mm diameter and placed on the geometry with a 1 mm gap. A thin layer of paraffin oil was applied around the sample and the geometry. The G' and G'' moduli were analyzed by heating samples from 1 to 40°C at a rate of 0.5°C.min^{-1} and the melting point was determined.

2.5. Biochemical and structural analyses

2.5.1. Determination of cross-linking degree

The formation of covalent bonds during cross-linking was estimated by the quantification of free amines with an OPA procedure according to Nielsen *et al.* (2001) with slight modifications. Briefly, an OPA solution was prepared daily with 25 mL of 0.1 M sodium tetraborate, 2.5 mL of 20% (w/v) SDS, 40 mg of OPA in 1 mL of absolute ethanol, 100 µL of BME and distilled water to a final volume of 50 mL (Church et al. 1983). Gelatin sponges (0.2 g) were solubilized in 2 mL of distilled water at 90°C for 1 h. Then, 50 µL of the mixture were homogenized in 1 mL of OPA reagent, 250 µL were deposited in triplicate in a 96-well microplate (Greiner Bio-One, Germany) and incubated 2 min at room temperature in the dark (Marco and Rosell 2008). The absorbance was determined at 340 nm with a spectrophotometer SPECTROstar Omega (BMG Labtech, Germany) using distilled water as control and a standard range of L-Leucine (from 0.5 to 5 mM). Cross-linking degree was calculated as: Cross-linking degree (%) = 100 – (% free amines compared to the native).

2.5.2. Microstructural analyses

The microstructural analyses of gelatin sponges were carried out by scanning electron microscopy (SEM) (Hitachi S-3200N, Germany) (PIMM core facility, University of Western Brittany, France). All samples (d: 26 mm × h: 10 mm) were cut in the center in the vertical plane and were fixed to a support to be coated with gold/palladium under vacuum. Pore size measurements (n = 10 per sample with two perpendicular measurements each) were conducted randomly from SEM images (Murphy et al. 2010; Krieghoff et al. 2019; Zamani et al. 2021).

2.5.3. Chemical composition

A small piece of gelatin sponge was cut and used for Fourier-transform infrared spectrometer (FTIR) analysis with a FT/IR-4600 spectrometer and IRT-5200 microscope (Jasco, France). The reflectance signal was collected on the region from 400 to 4000 cm^{-1} for 32 scans at a resolution of 4 cm^{-1}.

2.6. Material stability

2.6.1. Hydrogel stability and syneresis

The hydrogel stability and syneresis were determined by using a sample of 5 mL (diameter 2.6 cm) weighed (W0) and sealed on a sterile Petri dish. Samples were heated at 40°C for 24 h and 7 days. After this, hydrogels were wiped with absorbent paper to remove excess liquid and reweighed (Wf). The syneresis percentage was calculated as follows: Syneresis (%) = (W0 - Wf) / W0 x 100.

2.6.2. Sponge stability and water binding capacity

The water binding capacity was analysed for sponges according to Elango *et al*. (2016) with slight modifications. Briefly, the dried sample was weighed (Wd) before being sealed in a cup containing 5 mL of phosphate buffer 0.1 M (pH 6). After shaking, the cup was heated at 40°C for 7 days. Then, the wet sample was wiped to remove excess liquid, and weighed (Ww_1). The sample was returned to the cup and 5 mL of fresh phosphate buffer were added to extend the test to 30 days. At the end, the wet sample was wiped and weighed again (Ww_2). The water binding capacity was calculated as: Water binding capacity (%) = (Ww - Wd) / Wd x 100.

2.7. Statistical analyses

Results were expressed as mean ± standard deviation (SD) from three independent trials. The significance of differences was determined by Analysis of variance (ANOVA) and the multiple comparison was performed by Tukey's test. Statistical analyses were carried out with the software R (v. 3.6.1) and data with $P < 0.05$ were considered as statistically significant.

3. Results and discussion

3.1. Material characterization

3.1.1. Proximate analysis

Proximate composition presented in Table 2 allows to characterize the salmon gelatin material before the cross-linking procedure. Salmon gelatin contained mainly proteins (93.6%) with low moisture (7.1%), fat (1.2%) and ash (1.9%) contents confirming the effectiveness of the protein extraction.

3.1.2. SDS-polyacrylamide gel electrophoresis

The first approach to characterize the native material was the determination of the molecular weight distribution of S-NAT by means of SDS-PAGE under reducing conditions in comparison to P-NAT (Fig. 1). Both samples displayed two bands close to 250 kDa and two close bands with molecular weights of 118 and 108 kDa for S-NAT, and 130 and 117 kDa for P-NAT. These bands are characteristic of protein patterns of gelatin from collagen type I, namely two β-component (β11 and β12) about 245 kDa and two α-chains, α1 and α2, between 101-120 kDa as previously published in literature on salmon with other extraction methods (Chiou et al. 2006; Moreno et al. 2012; Alves et al. 2017; Díaz-Calderón et al. 2017). This electrophoresis profile confirmed the presence of gelatin in the salmon material obtained by thermal extraction and that both gelatin contained natural crosslinks by the presence of β-component. In fact, the α-chains are the basic units of gelatin and can connect by hydrogen bonds to form a β-component (a dimer) or γ-triple helix (a trimer, not detected) (Gomez-Guillén et al. 2001; Cheng et al. 2019). The increase in temperature disturbed the gelatin structures and

the addition of denaturing products broke the bonds that released the β-component and α-chains. Both samples had an α1 band more pronounced than the α2 band, as there is twice more α1 than α2 in the triple helix (Ahmad et al. 2010). S-NAT has lower molecular weights than P-NAT which may be due to a different amino acid composition (Chiou et al. 2006; Silva et al. 2014).

3.1.3. Size-exclusion chromatography

Native gelatins were characterized by SEC-HPLC to separate them on the basis of their size while preserving their conformation. The chromatographic patterns and distribution are shown in Fig. 2 and Table 3. Both gelatins presented a high proportion of molecular weight above 300 kDa, 68.57% for S-NAT and 77.07% for P-NAT. This high molecular weight of 300 kDa reflects the presence of α-chain aggregates under coil or triple helix structures corresponding to a preservation of the tertiary structure of these native gelatin (Djabourov 1991; Gomez-Guillén et al. 2001; Bode et al. 2011; Cheng et al. 2019). This difference with the SDS-PAGE results can be explained by the absence of denaturing conditions, so the weak bonds and the tertiary structures were preserved. The lower content of high molecular weight of S-NAT can be explained by a lower amount of intra- and inter-molecular cross-linked, resulting from a different amino acid composition (Haug and Draget 2011). However, non-denatured S-NAT was a promising candidate for enzymatic cross-linking as MTG produces higher molecular weight polymers by catalysing new cross-links (Huang et al. 2019).

3.1.4. Amino acid composition

The amino acid profiles of native gelatin were established in order to better understand the previous differences recorded in molecular weight distributions and the following rheological measurements (Table 4). Profiles revealed a wide variety of amino acids. The main amino acids of S-NAT and P-NAT were glycine (23.10% and 21.61% respectively), proline (11.06% and 13.66% respectively) and hydroxyproline (7.24% and 11.30% respectively). Glycine was present in high concentration as this small amino acid occurs at every third amino acid in the helical domain of an α chain allowing compact triple helices (Bhagwat and Dandge 2018; Huang et al. 2019). The amount of glycine can vary between 20-36% for mammalian gelatin or cold fish gelatin (including salmon) depending on the extraction technique (Arnesen and Gildberg 2007; Eysturskard et al. 2009; Acevedo et al. 2015; Díaz-Calderón et al. 2017). Proline and hydroxyproline are the amino acids most often cited to complete the triplet sequences with glycine. These both amino acids were in a higher proportion in P-NAT (24.96% combined) than in S-NAT (18.30% combined) which is close to literature (Arnesen and Gildberg 2007; Ferraro et al. 2010; Acevedo et al. 2015). This promotes the creation of bonds and may explain the higher proportions of high molecular weight for P-NAT than for S-NAT (Gómez-Estaca et al. 2009; Ferraro et al. 2010). Moreover, proline and hydroxyproline are also considered responsible for the resistance of gelatin and a lower concentration in S-NAT than in P-NAT would imply lower thermostability and bloom degree (Gomez-Guillén et al. 2001; Silva et al. 2014; Annamalai et al. 2019; Huang et al. 2019).

3.2. Rheological results

3.2.1. State transitions of native gelatins (sol-gel and gel-sol)

Linear viscoelastic properties of native gelatins were measured to determine the temperatures of state transitions. Samples were first cooled and the sol-gel transition, corresponding to G' = G", was shown to occur at

5.0 ± 1.0°C for S-NAT and at 23.6 ± 0.1°C for P-NAT, as illustrated in Fig. 3A. The gelation is a non-instantaneous process; first, the gelatin molecules change from a coil conformation to a helix by the random formation of hydrogen bonds. The gel is then formed when sufficient helicoidal regions are produced (Chen and Shi 2013). Helices will grow and stabilize the structure through crystal junction zones (Achet and He 1995; Chen and Shi 2013). The time-induced gel structurating is rheologically characterized by a sharp increase of the storage modulus G', from about 1 Pa at the gelling point for both S-NAT and P-NAT (Fig. 3A), to 1146.9 ± 952.4 Pa for S-NAT and 1170.7 Pa for P-NAT after one hour equilibration, highlighting the significant enhancement of gel elastic properties with time (Arnesen and Gildberg 2007). Gelatin is a material with a thermoreversible nature, when heated, the material loses cohesion and a gel-sol transition is obtained. S-NAT showed a lower thermal resistance than P-NAT with melting point at 16.7 ± 1.1°C and at 33.2°C, respectively (Fig. 3B). Ionic forces, pH, triple helix rate or molecular weight can impact the processes of state change (Djabourov et al. 1988a). Thus, the differences between S-NAT and P-NAT could be due to the higher amount of proline and hydroxyproline in P-NAT that are favorable to nucleation due to their stiffness (Djabourov 1988; Arnesen and Gildberg 2007). The adaptation to the body temperature has also a role in these differences as salmon is an ectothermic, living at 6-16°C, its temperature is lower than the temperature of terrestrial mammals (Jongjareonrak et al. 2006; Haug and Draget 2011; Diogo et al. 2021).

3.2.2. Cross-linking impact on thermal resistance

Sample thermal resistance after cross-linking was rheologically studied by analyzing G', G" as a function of temperature, as presented in Fig. 4 and Fig. 5. Melting temperatures of S-NAT and S-MTG2 were respectively 17.5 ± 0.3°C and 20.7 ± 0.1°C. The results showed that a weak network has developed in S-MTG2, but still not efficient enough to suppress the thermoreversibility of the material at the higher tested temperatures (Fig. 4). A study on the hoki fish gelatin has shown a similar increase of the melting temperature by 4.5°C with enzyme addition (Mohtar et al. 2013). The storage modulus G' of both S-MTG5 and S-MTG10 were shown to slightly decrease in the vicinity of the melting temperature of S-NAT, which could be due to the breaking of a weak physical network, with non-covalent cross-links present at low temperatures (Bode et al. 2011; Da Silva et al. 2014). However, the results show that the elastic properties were maintained at 40°C, due to the presence of a network with covalent cross-links (De Carvalho and Djabourov 1997; Bode et al. 2011). This loss of thermoreversibility was also obtained on porcine gelatin with the three enzyme concentrations (Fig. 5). Other studies on porcine gelatin cross-linked with MTG at 10 or 12 $U.g^{-1}$ of gelatin, showed an increase of the melting temperature above 50°C (Chen et al. 2003; Liu et al. 2020).

For both gelatins, the results plotted in Fig. 4 and Fig. 5 showed that enzymatic cross-linking result in hydrogels that were as mechanically and thermally resistant at 40°C as hydrogels obtained by chemical cross-linking. However, the G' modulus at 40°C of S-GTA (139.2 ± 14.6 Pa) is four times lower than that of S-MTG10.

Moreover, it is interesting to note that S-MTG10 exhibited elastic properties similar to those of P-MTG5 and P-MTG10 at 40°C, meaning that, above a given enzyme concentration threshold, marine gelatin could provide similar mechanical characteristics to those of mammalian gelatin and thus be a relevant substitute.

3.3. Biochemical and structural analyses

3.3.1. Determination of cross-linking degree

The sample cross-linking degrees were estimated based on the free amines in comparison to native gelatin with the OPA procedure; results are shown in Fig. 6, some data were obtained in a heterogeneous environment due to cross-linking. For salmon gelatin, the degree of cross-linking showed a significant increase for S-MTG5, S-MTG10 and S-GTA where covalent networks had developed to more than 70% of free amines. Overall, S-MTG5 and S-MTG10 developed a network of covalent bonds as rich as P-MTG2, P-MTG5 and even P-MTG10 for S-MTG10. Cross-linking degree seemed to reach a plateau between 70-85% at the enzyme concentrations tested. This can be explained by the progressive reduction of intermolecular space due to new covalent bonds that would have limited the mobility of the enzyme and its interaction with the entire substrate (Elango et al. 2016; Cheng et al. 2019). This is in contrast to chemical cross-linking, which was faster with the small size of the GTA and its diversity of action sites accepting more amino acids (Chatterji 1989; Barnes et al. 2007; Huang et al. 2019). The degree of cross-linking reached in our study was higher than 98%. By comparing rheology results, 70% of amino groups involved in the bonding network seem enough to obtain a cohesive and resistant material at 40°C for both gelatins.

3.3.2. Microstructural analyses

Microstructural analyses of gelatin sponges are necessary to know the pore size and shape. These parameters are important as they affect the functional and mechanical properties of the material (Song et al. 2006). SEM images show that all native and enzymatically cross-linked salmon gelatins possessed porous structures with interconnected cavities (Fig. 7). This feature is important as it allows diffusion of oxygen, nutrients, and liquid into the matrix (Song et al. 2006; Bermueller et al. 2013). SEM image analysis was used to determine the average pore size (Table 5). Pore size was significantly impacted by cross-linking in the S-MTG10 sponges. Indeed, the pores decreased from an average diameter of 720 ± 287 µm for S-NAT, to 461 ± 233 µm for S-MTG10 by the increase of the internal network. A decrease in pore size was also observed on bovine collagen following the addition of MTG (Cheng et al. 2019). The pore size influences the diffusion within the material. For potential medical applications as tissue substitute, the diameter of S-MTG10 seems to be the most appropriate for cell development as previous studies done on mammalian collagen sponges have concluded that pores between 300 and 500 µm are favorable to development of primary mesenchymal stem cells and osteoblasts (Murphy et al. 2016; Krieghoff et al. 2019). This diameter allows the development of tissue due to its large interface between the material and the cells. The pore shapes were irregular from round to flattened and the homogeneity of the material was increased concomitantly with the augmentation of enzyme's amount. Enzymatic cross-linking allows to modify the internal structure of the material to adapt it to the needs of future applications in terms of shape and pore size.

3.3.3. Chemical composition

The chemical structures of the sponges were analyzed by FTIR to observe the changes brought by cross-linking (Fig. 8). The sponges had a protein structure characterized by amide peaks. The peaks were located as follows: amide I about 1700-1600 nm (corresponds to C=O stretching vibrations), amide II about 1590-1500 nm (corresponds to C-N stretching coupled with N-H bending), amide III about 1200 nm (corresponds to C-N stretching coupled with N-H bending), amide A about 3295 nm (corresponds to N-H stretching coupled

with hydrogen bound) and amide B about 2900-2920 nm (corresponds to CH3 and CH2 asymmetric stretching) (Ahmad et al. 2017; Cheng et al. 2019).

The wavelengths of the peaks did not vary significantly between samples in contrast to their relative absorbance (Table 6). The major differences appeared to be on amides II and III with decreases in absorbance for S-MTG10 and S-GTA. The absorbance decrease for amide II reflects a change from NH_2 to NH through the creation of covalent intermolecular bonds between gelatin molecules for enzymatic cross-linking or between gelatin molecules and GTA for chemical cross-linking (Chen et al. 2014). The absorbance decrease for amide III reflects a decrease in the amount of triple helices. The creation of new covalent bonds disrupted the formation of triple helices during cooling, which remained partially coiled (Cheng et al. 2019). Furthermore, it has been shown that an amide III and 1450 nm ratio close to 1 indicates a triple helix structure, but this ratio decreased, in comparison to the native gelatin, when the enzyme concentration increased, proving the partial loss of the triple helices (Ahmad et al. 2010; Zhang et al. 2016). The rheological differences between S-MTG5 and S-MTG10 seemed to be explained by a different internal chemical structure, the covalent bonds were not formed in the same way. It appears that S-MTG5 had an intramolecular network with triple helix structures formed by covalent bonds because amide II and III absorbances were close to those of S-NAT while S-MTG5 had acquired high thermal and mechanical resistances.

3.4. Biomaterial stability

3.4.1. Hydrogel stability and syneresis

The hydrogels were macroscopically identical with the exception of S-GTA that showed an orange color in contrast to the white color of the others (Fig. 9). This coloration is due to the consumption of aldehyde groups during chemical cross-linking, which does not occur with the enzyme (Chatterji 1989; Tian et al. 2016).

The hydrogels were maintained for 7 days at 40°C to mimic an ageing process of the material in order to observe their stability on a longer period and with larger samples than rheological analyses (Fig. 9). Their ability to retain their hydration was also analyzed (Fig. 10). Indeed, in some domains of applications such as wound healing dressing or more broadly in tissue engineering, it is necessary for a hydrogel to maintain its structure as well as its hydration, because this influences the permeability to nutrients and potentially its biocompatibility (Zhao et al. 2016). S-NAT was completely liquefied in less than 1h30 that confirmed its thermoreversible ability. S-MTG2 remained solid at 40°C, contrary to rheological analyses for 7 days (Fig. 4). Possible explanations for this are the absence of applied mechanical stress, the higher thickness of the sample or the slight drying of the hydrogel surface that maintained the structure. However, the structure of S-MTG2 was not completely cohesive; it was difficult to handle due to a high viscosity. S-MTG5, S-MTG10 and S-GTA retained their original gel form, which confirmed their acquisition of a durable thermal resistance. However, S-MTG5 and S-MTG10 had different behaviors at the end of the test, S-MTG5 was viscous and sticky while S-MTG10 was more rigid and not sticky that can be explained by the FTIR data, which showed different modifications in chemical structures (Fig. 8).

Concerning syneresis, S-MTG5 showed the lowest rates (around 8-15%) which did not vary significantly over the analysis period (Fig. 10). S-MTG10 released more liquid after 7 days showing a more developed hydrophobicity, because during the cross-linking reaction, hydrophilic amino acids of the gelatin were used to form the bonds (Liu et al. 2020). This hydrophobic effect was accentuated for S-GTA with higher and faster

syneresis (34% in 24 h and 46% in 7 days) due to its higher cross-linking degree (Chen et al. 2014). These differences in behavior can offer versatility in applications to the material depending on the amount of enzyme used.

3.4.2. Sponge stability and water binding capacity

The stability of the gelatin sponges in rehydration conditions at 40°C was assessed in order to better understand the impact of freeze-drying (Fig. 11). All the cross-linked sponges retained a solid state over the period of analysis, including S-MTG2, which implies that freeze-drying strengthened its structure (Schoof et al. 2001; Buttafoco et al. 2006). Buffer turnover during the analysis did not affect the swelling rates as shown in Fig. 12. S-MTG2 and S-MTG5 showed swelling rates of 630-690% while lower water binding capacities were observed for S-MTG10 and S-GTA with swelling rates of 350-450%. Their higher hydrophobic abilities are explained by the increase of their molecular weights due to the formation of covalent bonds and the loss of hydrophilic sites (Chen et al. 2014; Huang et al. 2019; Liu et al. 2020). These different degrees of water binding capacities are promising. Indeed, the materials could go through a freeze-drying step to facilitate their preservation and then be rehydrated before its use.

4. Conclusion

This study demonstrated the effect of enzymatic cross-linking by microbial transglutaminase (MTG) on Atlantic salmon skin gelatin. The result was a potential porous gelatin-based biomaterial for various applications by its structure, its mechanical and thermal resistances and its water conservation capacity. This enzyme-assisted modification improved the mechanical and thermal resistances of the gelatin. Depending on the amount of enzyme used, it was possible to adapt the properties of the biomaterial to different potential applications. A cross-linking with 5% enzyme (6.25 $U.g^{-1}$ of gelatin) allowed the development of a sticky and viscous material that may be interesting as cosmetic patch or wound healing dressing, while the addition of 10% enzyme (12.5 $U.g^{-1}$ of gelatin) allowed to obtain a rigid and non-sticky material interesting as packaging for food or scaffold for tissue engineering. Moreover, both biomaterials were resistant to temperatures above 40°C and to rehydration. This work is a premise for future work that should focus on cellular analysis to test its ability to support bone-marrow mesenchymal stem cells survival and its biocompatibility, as well as its degradation. Complementary mechanical tests such as compressive and tensile strength analyses must also be performed to use it in the medical field as tissue substitute.

CRediT authorship contribution statement

Buscaglia M.: Conceptualization, Methodology, Investigation, Formal analysis, Writing - Original draft preparation and Writing - Review & Editing. **Guerard F.**: Conceptualization, Methodology, Formal analysis, Writing - Review & Editing, Supervision and Funding acquisition. **Roquefort P.**: Methodology, Investigation and Formal analysis. **Aubry T.**: Conceptualization, Writing - Review & Editing. **Fauchon M.**: Investigation. **Toueix Y.**: Investigation. **Stiger-Pouvreau V.**: Writing - Review & Editing, Supervision and Funding acquisition. **Hellio C.**: Writing - Review & Editing, Supervision and Funding acquisition. **Le Blay G.**: Writing - Review & Editing, Supervision and Funding acquisition.

Declaration of competing interest

The authors declare that they have no known competing financial interests or personal relationships that could have appeared to influence the work reported in this paper.

Acknowledgments

This study was financially supported by the European Union through the INTERREG Atlantic Programme, under the scope of BLUEHUMAN (EAPA_151/2016) project. This work was also supported by Biogenouest through the Biodimar team (LEMAR, UBO). The PhD fellowship of Manon Buscaglia was funded by the Conseil Regional de Bretagne (ARED N°585) and the European Union through the INTERREG Atlantic Programme, under the scope of BLUEHUMAN (EAPA_151/2016).

Data availability

Methods, materials, and data used in this study are fully delineated in the text.

References

Acevedo CA, Diáz-Calderón P, López D, Enrione J (2015) Assessment of gelatin-chitosan interactions in films by a chemometrics approach. CYTA - J Food 13:227–234. https://doi.org/10.1080/19476337.2014.944570

Acevedo CA, Sánchez E, Orellana N, et al (2019) Re-epithelialization appraisal of skin wound in a porcine model using a salmon-gelatin based biomaterial as wound dressing. Pharmaceutics 11:. https://doi.org/10.3390/pharmaceutics11050196

Achet D, He XW (1995) Determination of the renaturation level in gelatin films. Polymer (Guildf) 36:787–791. https://doi.org/10.1016/0032-3861(95)93109-Y

Adamiak K, Sionkowska A (2020) Current methods of collagen cross-linking: Review. Int J Biol Macromol 161:550–560. https://doi.org/10.1016/j.ijbiomac.2020.06.075

Ahmad M, Benjakul S, Nalinanon S (2010) Compositional and physicochemical characteristics of acid solubilized collagen extracted from the skin of unicorn leatherjacket (*Aluterus monoceros*). Food Hydrocoll 24:588–594. https://doi.org/10.1016/j.foodhyd.2010.03.001

Ahmad T, Ismail A, Ahmad SA, et al (2017) Recent advances on the role of process variables affecting gelatin yield and characteristics with special reference to enzymatic extraction: A review. Food Hydrocoll 63:85–96. https://doi.org/10.1016/j.foodhyd.2016.08.007

Alves AL, Marques ALP, Martins E, et al (2017) Cosmetic Potential of Marine Fish Skin Collagen. Cosmetics 1–16. https://doi.org/10.3390/cosmetics4040039

Annamalai RT, Hong X, Schott NG, et al (2019) Injectable osteogenic microtissues containing mesenchymal

stromal cells conformally fill and repair critical-size defects. Biomaterials 208:32–44. https://doi.org/10.1016/j.biomaterials.2019.04.001

Arnesen JA, Gildberg A (2007) Extraction and characterisation of gelatine from Atlantic salmon (*Salmo salar*) skin. Bioresour Technol 98:53–57. https://doi.org/10.1016/j.biortech.2005.11.021

Bae I, Osatomi K, Yoshida A, et al (2008) Biochemical properties of acid-soluble collagens extracted from the skins of underutilised fishes. Food Chem 108:49–54. https://doi.org/10.1016/j.foodchem.2007.10.039

Barnes CP, Pemble IV CW, Brand DD, et al (2007) Cross-linking electrospun type II collagen tissue engineering scaffolds with carbodiimide in ethanol. Tissue Eng 13:1593–1605. https://doi.org/10.1089/ten.2006.0292

Battisti R, Fronza N, Vargas Júnior Á, et al (2017) Gelatin-coated paper with antimicrobial and antioxidant effect for beef packaging. Food Packag Shelf Life 11:115–124. https://doi.org/10.1016/j.fpsl.2017.01.009

Bello AB, Kim D, Kim D, et al (2020) Engineering and functionalization of gelatin biomaterials: From cell culture to medical applications. Tissue Eng - Part B Rev 26:164–180. https://doi.org/10.1089/ten.teb.2019.0256

Berendt AR, Peters EJG, Bakker K, et al (2008) Diabetic foot osteomyelitis: a progress report on diagnosis and a systematic review of treatment. Diabetes Metab Res Rev 24:S145–S161. https://doi.org/10.1002/dmrr.836

Bermueller C, Schwarz S, Elsaesser AF, et al (2013) Marine collagen scaffolds for nasal cartilage repair: Prevention of nasal septal perforations in a new orthotopic rat model using tissue engineering techniques. Tissue Eng - Part A 19:2201–2214. https://doi.org/10.1089/ten.tea.2012.0650

Bhagwat PK, Dandge PB (2018) Collagen and collagenolytic proteases: A review. Biocatal Agric Biotechnol 15:43–55. https://doi.org/10.1016/j.bcab.2018.05.005

Bigi A, Cojazzi G, Panzavolta S, et al (2001) Mechanical and thermal properties of gelatin films at different degrees of glutaraldehyde crosslinking. Biomaterials 22:763–768. https://doi.org/10.1016/S0142-9612(00)00236-2

Bode F, Da Silva MA, Drake AF, et al (2011) Enzymatically cross-linked tilapia gelatin hydrogels: Physical, chemical, and hybrid networks. Biomacromolecules 12:3741–3752. https://doi.org/10.1021/bm2009894

Broderick EP, O'Halloran DM, Rochev YA, et al (2005) Enzymatic stabilization of gelatin-based scaffolds. J Biomed Mater Res - Part B Appl Biomater 72:37–42. https://doi.org/10.1002/jbm.b.30119

Buttafoco L, Engbers-Buijtenhuijs P, Root AA, et al (2006) First steps towards tissue engineering of small-diameter blood vessels: preparation of flat scaffolds of collagen and elastin by means of freeze drying. J Biomed Mater Res - Part B Appl Biomater 77:357–368. https://doi.org/10.1002/jbm.b.30444

Charulatha V, Rajaram A (2003) Influence of different crosslinking treatments on the physical properties of collagen membranes. Biomaterials 24:759–767. https://doi.org/10.1016/S0142-9612(02)00412-X

Chatterji PR (1989) Gelatin with hydrophilic/hydrophobic grafts and glutaraldehyde crosslinks. J Appl Polym Sci 37:2203–2212. https://doi.org/10.1002/app.1989.070370812

Chau DYS, Collighan RJ, Verderio EAM, et al (2005) The cellular response to transglutaminase-cross-linked collagen. Biomaterials 26:6518–6529. https://doi.org/10.1016/j.biomaterials.2005.04.017

Chen MM, Huang YQ, Guo H, et al (2014) Preparation, characterization, and potential biomedical application of composite sponges based on collagen from silver carp skin. J Appl Polym Sci 131:1–8. https://doi.org/10.1002/app.40998

Chen RN, Ho HO, Sheu MT (2005) Characterization of collagen matrices crosslinked using microbial

transglutaminase. Biomaterials 26:4229–4235. https://doi.org/10.1016/j.biomaterials.2004.11.012

Chen T, Embree HD, Brown EM, et al (2003) Enzyme-catalyzed gel formation of gelatin and chitosan: Potential for in situ applications. Biomaterials 24:2831–2841. https://doi.org/10.1016/S0142-9612(03)00096-6

Chen X, Shi Q (2013) Research on sol-gel transition process of gelatin. Adv Mater Res 683:474–478. https://doi.org/10.4028/www.scientific.net/AMR.683.474

Cheng S, Wang W, Li Y, et al (2019) Cross-linking and film-forming properties of transglutaminase-modified collagen fibers tailored by denaturation temperature. Food Chem 271:527–535. https://doi.org/10.1016/j.foodchem.2018.07.223

Chiou B Sen, Avena-Bustillos RJ, Shey J, et al (2006) Rheological and mechanical properties of cross-linked fish gelatins. Polymer (Guildf) 47:6379–6386. https://doi.org/10.1016/j.polymer.2006.07.004

Church FC, Swaisgood HE, Porter DH, Catignani GL (1983) Spectrophotometric Assay Using o-Phthaldialdehyde for Determination of Proteolysis in Milk and Isolated Milk Proteins. J Dairy Sci 66:1219–1227. https://doi.org/10.3168/jds.S0022-0302(83)81926-2

Commission E (2009) Commission regulation (EC) No 152/2009 of 27 January 2009 laying down the methods of sampling and analysis for the official control of feed. Off J Eur Union 1–130

Da Silva K, Kumar P, Van Vuuren SF, et al (2021) Three-Dimensional Printability of an ECM-Based Gelatin Methacryloyl (GelMA) Biomaterial for Potential Neuroregeneration. ACS Omega 6:21368–21383. https://doi.org/10.1021/acsomega.1c01903

Da Silva MA, Bode F, Drake AF, et al (2014) Enzymatically cross-linked gelatin/chitosan hydrogels: Tuning gel properties and cellular response. Macromol Biosci 14:817–830. https://doi.org/10.1002/mabi.201300472

De Carvalho RA, Grosso CRF (2004) Characterization of gelatin based films modified with transglutaminase, glyoxal and formaldehyde. Food Hydrocoll 18:717–726. https://doi.org/10.1016/j.foodhyd.2003.10.005

De Carvalho W, Djabourov M (1997) Physical gelation under shear for gelatin gels. Rheol Acta 36:591–609. https://doi.org/10.1007/BF00367355

Díaz-Calderón P, Flores E, González-Muñoz A, et al (2017) Influence of extraction variables on the structure and physical properties of salmon gelatin. Food Hydrocoll 71:118–128. https://doi.org/10.1016/j.foodhyd.2017.05.004

Diogo GS, Carneiro F, Freitas-Ribeiro S, et al (2021) *Prionace glauca* skin collagen bioengineered constructs as a promising approach to trigger cartilage regeneration. Mater Sci Eng C 120:. https://doi.org/10.1016/j.msec.2020.111587

Djabourov M (1988) Architecture of gelatin gels. Contemp Phys 29:273–297. https://doi.org/10.1080/00107518808224377

Djabourov M (1991) Gelation—A review. Polym Int 25:135–143. https://doi.org/10.1002/pi.4990250302

Djabourov M, Leblond J, Papon P (1988a) Gelation of aqueous gelatin solutions. I. Structural investigation. J Phys 49:319–332

Djabourov M, Leblond J, Papon P (1988b) Gelation of aqueous gelatin solutions. II. Rheology of the sol-gel transition. J Phys 49:333–343

Echave MC, Hernáez-Moya R, Iturriaga L, et al (2019) Recent advances in gelatin-based therapeutics. Expert Opin Biol Ther 19:773–779. https://doi.org/10.1080/14712598.2019.1610383

Ehrlich H (2015) Marine Gelatins. In: Biological Materials of Marine Origin. pp 343–359

Elango J, Zhang J, Bao B, et al (2016) Rheological, biocompatibility and osteogenesis assessment of fish collagen scaffold for bone tissue engineering. Int J Biol Macromol 91:51–59. https://doi.org/10.1016/j.ijbiomac.2016.05.067

Eysturskard J, Haug IJ, Elharfaoui N, et al (2009) Structural and mechanical properties of fish gelatin as a function of extraction conditions. Food Hydrocoll 23:1702–1711. https://doi.org/10.1016/j.foodhyd.2009.01.008

FAO (2020) La situation mondiale des pêches et de l'aquaculture 2020. La durabilité en action.

Ferraro V, Cruz IB, Jorge RF, et al (2010) Valorisation of natural extracts from marine source focused on marine by-products: A review. Food Res Int 43:2221–2233. https://doi.org/10.1016/j.foodres.2010.07.034

Folk JE (1970) Transglutaminase (Guinea Pig Liver). Methods Enzymol 17:889–894. https://doi.org/10.1016/0076-6879(71)17302-8

Gelse K, Pöschl E, Aigner T (2003) Collagens - Structure, function, and biosynthesis. Adv Drug Deliv Rev 55:1531–1546. https://doi.org/10.1016/j.addr.2003.08.002

Gómez-Estaca J, Montero P, Fernández-Martín F, Gómez-Guillén MC (2009) Physico-chemical and film-forming properties of bovine-hide and tuna-skin gelatin: A comparative study. J Food Eng 90:480–486. https://doi.org/10.1016/j.jfoodeng.2008.07.022

Gomez-Guillén MC, Sarabia AI, Solas MT, Montero P (2001) Effect of microbial transglutaminase on the functional properties of megrim (*Lepidorhombus boscii*) skin gelatin. J Sci Food Agric 81:665–673. https://doi.org/10.1002/jsfa.865

Gu L, Shan T, Ma Y xuan, et al (2019) Novel Biomedical Applications of Crosslinked Collagen. Trends Biotechnol 37:464–491. https://doi.org/10.1016/j.tibtech.2018.10.007

Harrington WF, Rao V (1970) Collagen Structure in Solution. I. Kinetics of Helix Regeneration in Single-Chain Gelatins. Biochemistry 9:3714–3724. https://doi.org/10.1021/bi00821a010

Haug IJ, Draget KI (2011) Gelatin. In: Handbook of Food Proteins. pp 92–115

Hemon M, Guérard F, Fagon R, et al (2016) Wo 2016/142633

Huang T, Tu Z cai, Shangguan X, et al (2019) Fish gelatin modifications: A comprehensive review. Trends Food Sci Technol 86:260–269. https://doi.org/10.1016/j.tifs.2019.02.048

Jongjareonrak A, Benjakul S, Visessanguan W, Tanaka M (2005) Isolation and characterization of collagen from bigeye snapper (*Priacanthus macracanthus*) skin. J Sci Food Agric 85:1203–1210. https://doi.org/10.1002/jsfa.2072

Jongjareonrak A, Benjakul S, Visessanguan W, Tanaka M (2006) Skin gelatin from bigeye snapper and brownstripe red snapper: Chemical compositions and effect of microbial transglutaminase on gel properties. Food Hydrocoll 20:1216–1222. https://doi.org/10.1016/j.foodhyd.2006.01.006

Karim AA, Bhat R (2009) Fish gelatin: properties, challenges, and prospects as an alternative to mammalian gelatins. Food Hydrocoll 23:563–576. https://doi.org/10.1016/j.foodhyd.2008.07.002

Krieghoff J, Picke AK, Salbach-Hirsch J, et al (2019) Increased pore size of scaffolds improves coating efficiency with sulfated hyaluronan and mineralization capacity of osteoblasts. Biomater Res 23:1–13. https://doi.org/10.1186/s40824-019-0172-z

Laemmli UK (1970) Cleavage of structural proteins during the assembly of the head of bacteriophage T4. Nature 227:680–685

Liu Y, Weng R, Wang W, et al (2020) Tunable physical and mechanical properties of gelatin hydrogel after transglutaminase crosslinking on two gelatin types. Int J Biol Macromol 162:405–413. https://doi.org/10.1016/j.ijbiomac.2020.06.185

Lv LC, Huang QY, Ding W, et al (2019) Fish gelatin: The novel potential applications. J Funct Foods 63:. https://doi.org/10.1016/j.jff.2019.103581

Marco C, Rosell CM (2008) Effect of different protein isolates and transglutaminase on rice flour properties. J Food Eng 84:132–139. https://doi.org/10.1016/j.jfoodeng.2007.05.003

Mohtar NF, Perera CO, Quek SY, Hemar Y (2013) Optimization of gelatine gel preparation from New Zealand hoki (*Macruronus novaezelandiae*) skins and the effect of transglutaminase enzyme on the gel properties. Food Hydrocoll 31:204–209. https://doi.org/10.1016/j.foodhyd.2012.10.011

Moreno HM, Montero MP, Gómez-Guillén MC, et al (2012) Collagen characteristics of farmed Atlantic salmon with firm and soft fillet texture. Food Chem 134:678–685. https://doi.org/10.1016/j.foodchem.2012.02.160

Morimura S, Nagata H, Uemura Y, et al (2002) Development of an effective process for utilization of collagen from livestock and fish waste. Prog Biochem 37:1403–1412

Murphy CM, Duffy GP, Schindeler A, O'Brien FJ (2016) Effect of collagen-glycosaminoglycan scaffold pore size on matrix mineralization and cellular behavior in different cell types. J Biomed Mater Res - Part A 104:291–304. https://doi.org/10.1002/jbm.a.35567

Murphy CM, Haugh MG, O'Brien FJ (2010) The effect of mean pore size on cell attachment, proliferation and migration in collagen-glycosaminoglycan scaffolds for bone tissue engineering. Biomaterials 31:461–466. https://doi.org/10.1016/j.biomaterials.2009.09.063

Nielsen PM, Petersen D, Dambmann C (2001) Improved method for determining food protein degree of hydrolysis. J Food Sci 66:642–646. https://doi.org/10.1111/j.1365-2621.2001.tb04614.x

Nitsuwat S, Zhang P, Ng K, Fang Z (2021) Fish gelatin as an alternative to mammalian gelatin for food industry: A meta-analysis. Lwt 141:110899. https://doi.org/10.1016/j.lwt.2021.110899

Prasad A (2021) State of art review on bioabsorbable polymeric scaffolds for bone tissue engineering. Mater Today Proc 44:1391–1400. https://doi.org/10.1016/j.matpr.2020.11.622

Schoof H, Apel J, Heschel I, Rau G (2001) Control of pore structure and size in freeze-dried collagen sponges. J Biomed Mater Res 58:352–357. https://doi.org/10.1002/jbm.1028

Silva TH, Moreira-Silva J, Marques ALP, et al (2014) Marine origin collagens and its potential applications. Mar Drugs 12:5881–5901. https://doi.org/10.3390/md12125881

Silvipriya KS, Krishna Kumar K, Bhat AR, et al (2015) Collagen: Animal sources and biomedical application. J Appl Pharm Sci 5:123–127. https://doi.org/10.7324/JAPS.2015.50322

Song E, Yeon Kim S, Chun T, et al (2006) Collagen scaffolds derived from a marine source and their biocompatibility. Biomaterials 27:2951–2961. https://doi.org/10.1016/j.biomaterials.2006.01.015

Stachel I, Schwarzenbolz U, Henle T, Meyer M (2010) Cross-linking of type I collagen with microbial transglutaminase: Identification of cross-linking sites. Biomacromolecules 11:698–705. https://doi.org/10.1021/bm901284x

Tian Z, Liu W, Li G (2016) The microstructure and stability of collagen hydrogel cross-linked by glutaraldehyde. Polym Degrad Stab 130:264–270. https://doi.org/10.1016/j.polymdegradstab.2016.06.015

Van Vlierberghe S, Vanderleyden E, Boterberg V, Dubruel P (2011) Gelatin functionalization of biomaterial

surfaces: Strategies for immobilization and visualization. Polymers (Basel) 3:114–130. https://doi.org/10.3390/polym3010114

Zamani Y, Amoabediny G, Mohammadi J, et al (2021) Increased osteogenic potential of pre-osteoblasts on three-dimensional printed scaffolds compared to porous scaffolds for bone regeneration. Iran Biomed J 25:78–87. https://doi.org/10.29252/ibj.25.2.78

Zhang Q, Wang Q, Lv S, et al (2016) Comparison of collagen and gelatin extracted from the skins of Nile tilapia (*Oreochromis niloticus*) and channel catfish (*Ictalurus punctatus*). Food Biosci 13:41–48. https://doi.org/10.1016/j.fbio.2015.12.005

Zhao L, Li X, Zhao J, et al (2016) A novel smart injectable hydrogel prepared by microbial transglutaminase and human-like collagen: Its characterization and biocompatibility. Mater Sci Eng C 68:317–326. https://doi.org/10.1016/j.msec.2016.05.108

Mechanically enhanced *Salmo salar* gelatin by enzymatic cross-linking: premise of a bioinspired material for food packaging, cosmetics and biomedical applications

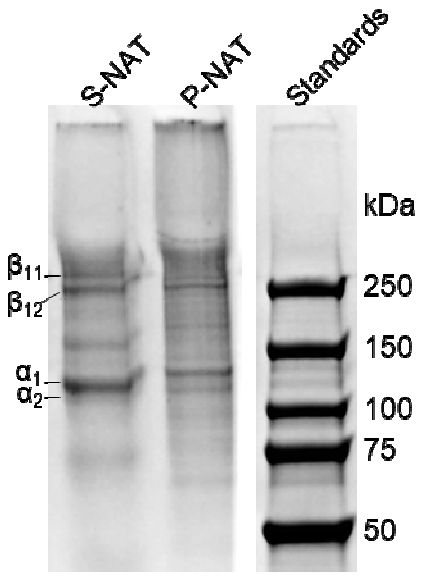

Fig. 1 SDS-PAGE profiles of the native gelatin samples. Lane 1: S-NAT: salmon native gelatin; lane 2: P-NAT: porcine native gelatin; lane 3: Standards (in kDa).

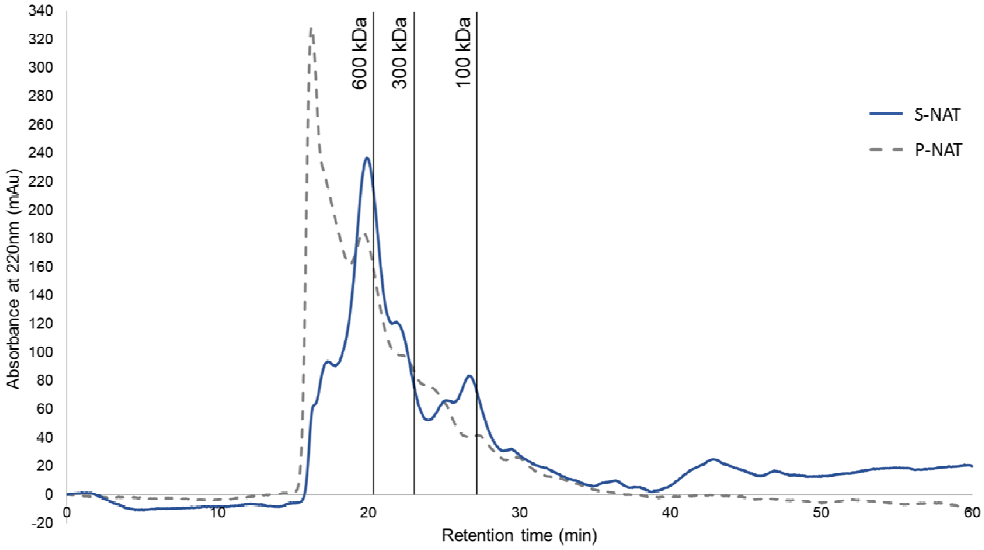

Fig. 2 SEC-HPLC profiles of the native gelatin samples. S-NAT: salmon native gelatin (continuous line) and P-NAT: porcine native gelatin (dashed line).

Mechanically enhanced *Salmo salar* gelatin by enzymatic cross-linking: premise of a bioinspired material for food packaging, cosmetics and biomedical applications

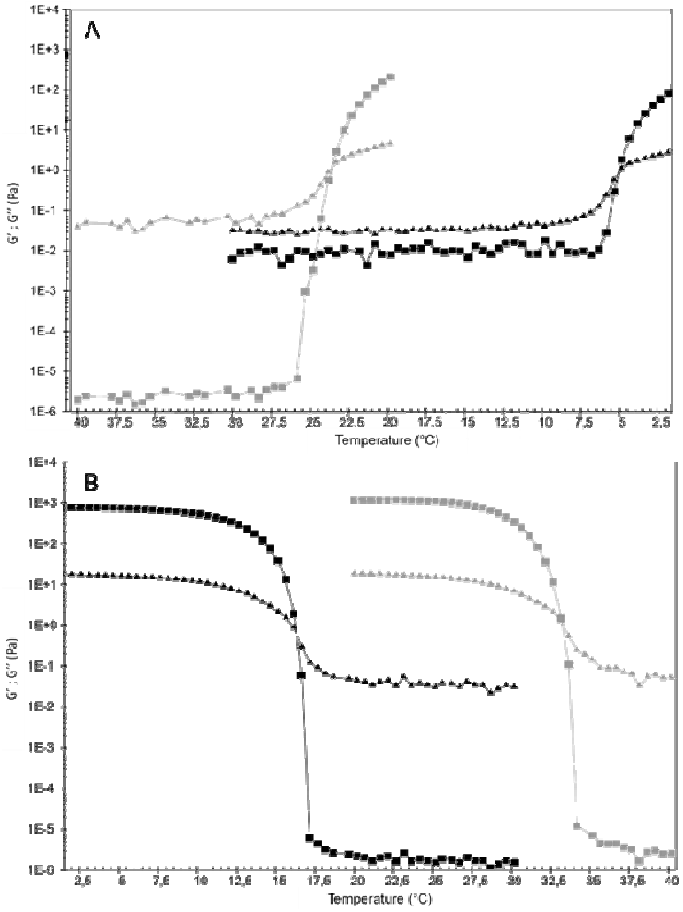

Fig. 3 State transitions of native gelatins. Storage modulus (G' - squares) and loss modulus (G" - triangles), at a frequency of 1 Hz in the linear regime, as a function of temperature for native salmon (S-NAT - in black) and porcine gelatins (P-NAT - in grey) (n = 3). A: gelling temperature analyses and B: melting temperatures analyses.

Mechanically enhanced *Salmo salar* gelatin by enzymatic cross-linking: premise of a bioinspired material for food packaging, cosmetics and biomedical applications

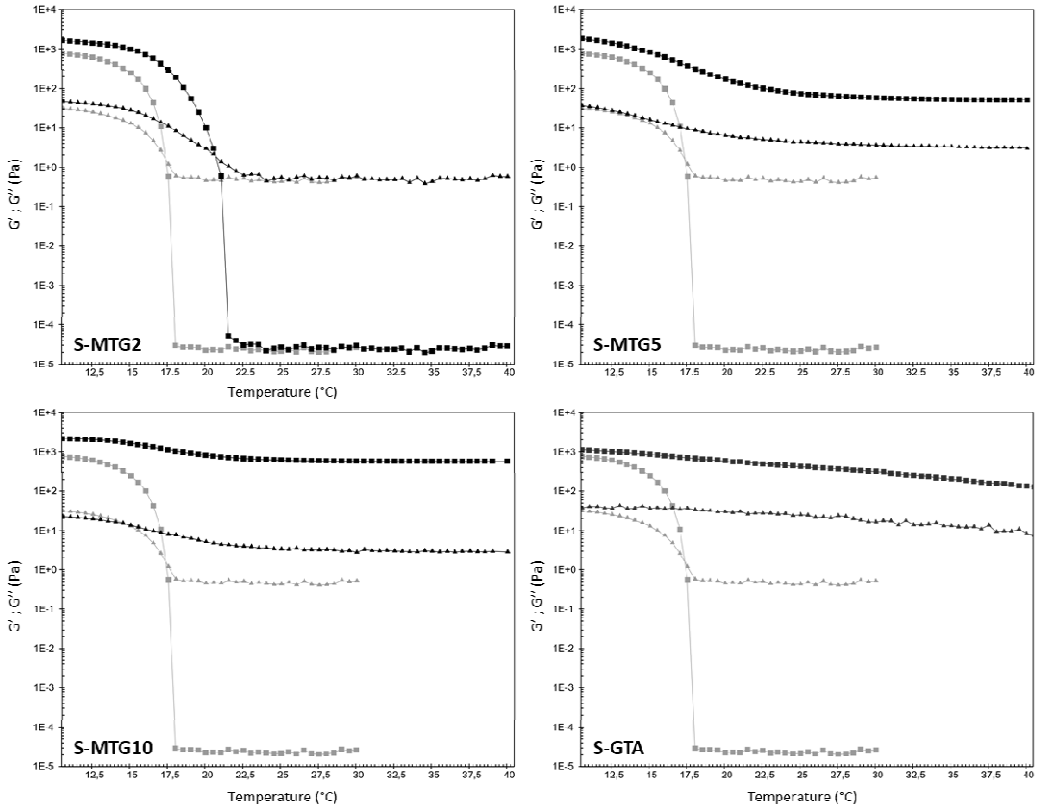

Fig. 4 Cross-linking impact on thermal resistance of salmon gelatin. Storage modulus (G' - squares) and loss modulus (G" - triangles), at a frequency of 1 Hz in the linear regime, as a function of heating temperature. Native gelatin is represented in light grey as control. S: salmon gelatin, MTG: enzymatically cross-linked gelatin (the associated number is the % of enzyme), and GTA: chemically cross-linked gelatin (n = 3).

Mechanically enhanced *Salmo salar* gelatin by enzymatic cross-linking: premise of a bioinspired material for food packaging, cosmetics and biomedical applications

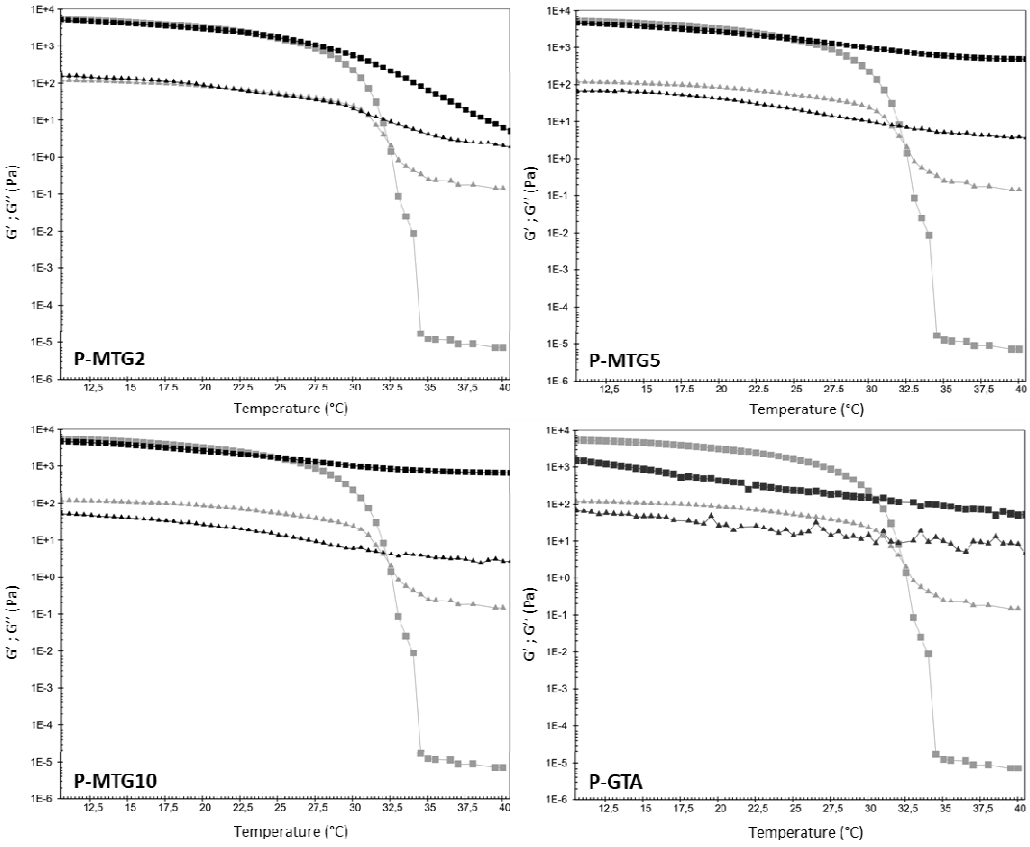

Fig. 5 Cross-linking impact on thermal resistance of porcine gelatin. Storage modulus (G' - squares) and loss modulus (G" - triangles), at a frequency of 1 Hz in the linear regime, as a function of heating temperature.. Native gelatin is represented in light grey as control. P: porcine gelatin, MTG: enzymatically cross-linked gelatin (the associated number is the % of enzyme), and GTA: chemically cross-linked gelatin (n = 3).

Mechanically enhanced *Salmo salar* gelatin by enzymatic cross-linking: premise of a bioinspired material for food packaging, cosmetics and biomedical applications

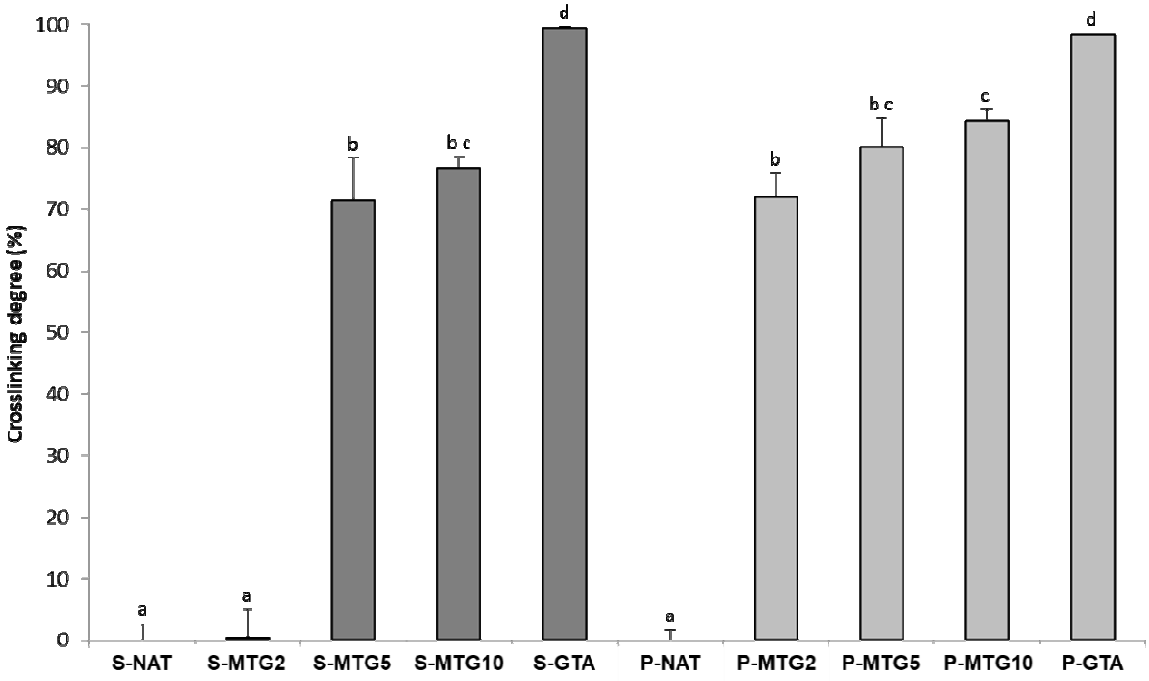

Fig. 6 Cross-linking degree (%) of native and cross-linked sponges for salmon (in dark grey) and porcine gelatins (in light grey) (n = 3). S: salmon gelatin, P: porcine gelatin, NAT: native gelatin, MTG: enzymatically cross-linked gelatin (the associated number is the % of enzyme), and GTA: chemically cross-linked gelatin. Different letters above the histogram bars indicate significant differences $P < 0.05$.

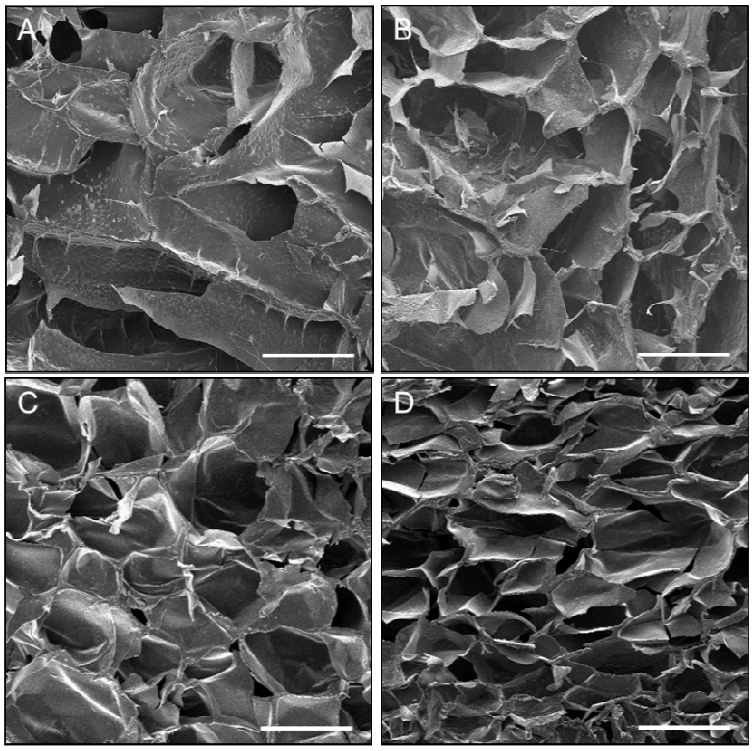

Fig. 7 Representative microstructures of vertical sections of gelatin sponges by SEM. (A) corresponds to S-NAT, (B) to S-MTG2, (C) to S-MTG5 and (D) to S-MTG10. S: salmon gelatin, NAT: native gelatin, and MTG: enzymatically cross-linked gelatin (the associated number is the % of enzyme). Scale bar: 1 mm.

Mechanically enhanced *Salmo salar* gelatin by enzymatic cross-linking: premise of a bioinspired material for food packaging, cosmetics and biomedical applications

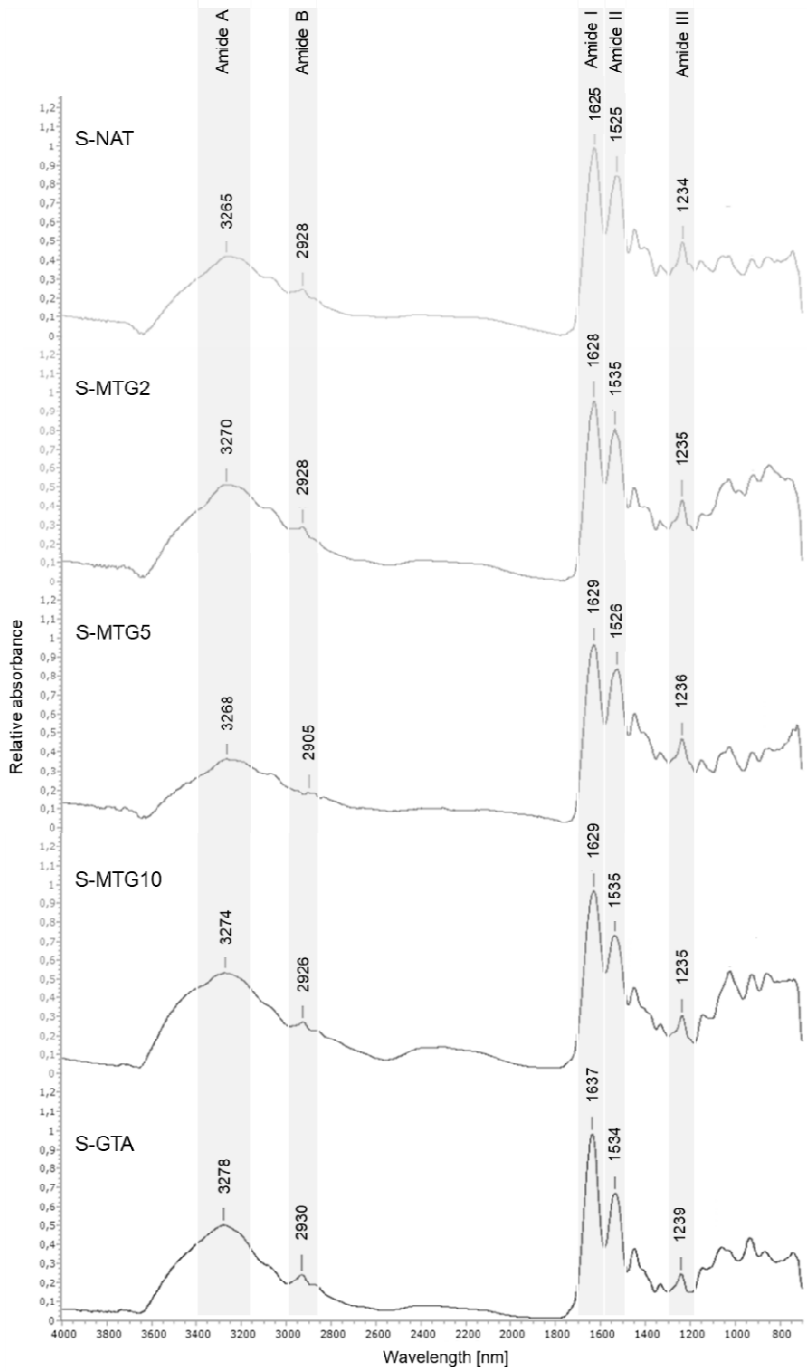

Fig. 8 FTIR spectra of the native and cross-linked samples of salmon gelatin (n = 3). S: salmon gelatin, NAT: native gelatin, MTG: enzymatically cross-linked gelatin (the associated number is the % of enzyme), and GTA: chemically cross-linked gelati

.

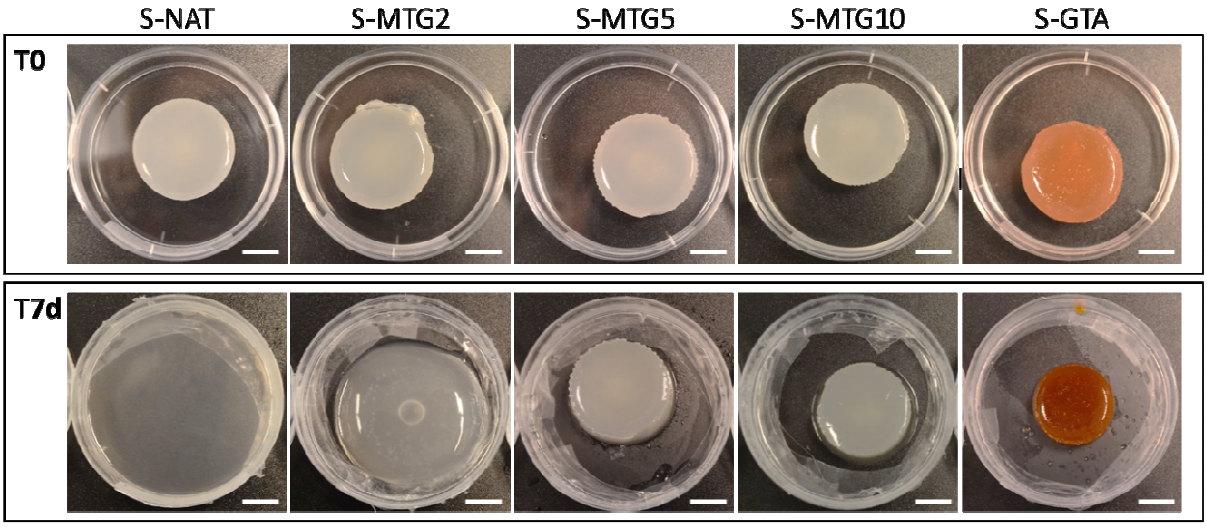

Fig. 9 Macroscopic demonstration of hydrogel stability after 7 days at 40°C (n = 3). S: salmon gelatin, NAT: native gelatin, MTG: enzymatically cross-linked gelatin (the associated number is the % of enzyme), and GTA: chemically cross-linked gelatin. Scale bar: 1 cm.

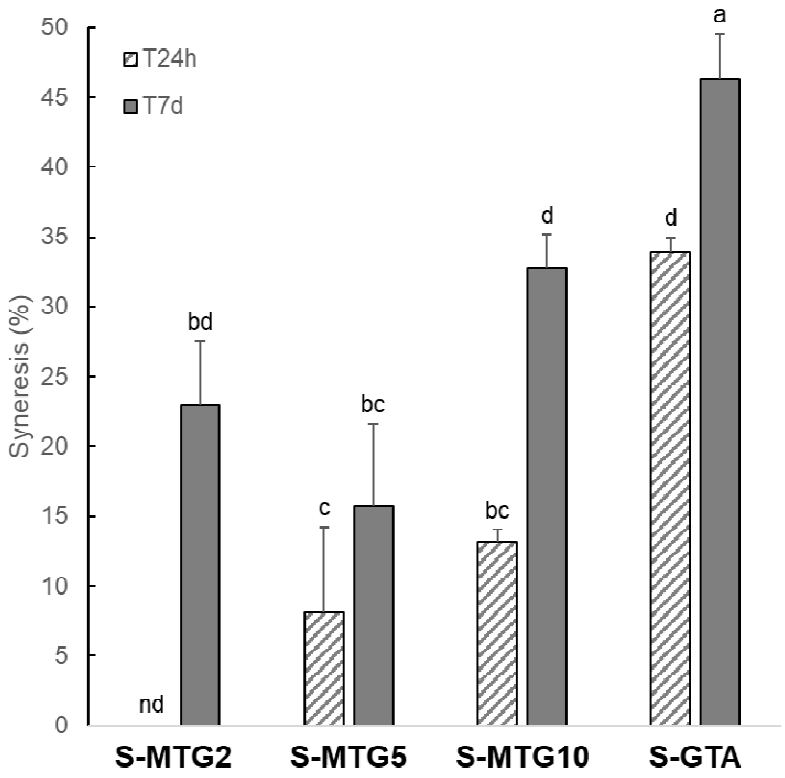

Fig. 10 Syneresis rate (%) of cross-linked salmon gelatin hydrogels after 24 h (T24h - hatched bars) and 7 days (T7d - filled bars) (n = 3). S: salmon gelatin, MTG: enzymatically cross-linked gelatin (the associated number is the % of enzyme), and GTA: chemically cross-linked gelatin. Different letters above the histogram bars indicate significant differences $P < 0.05$. nd: not determined.

Mechanically enhanced *Salmo salar* gelatin by enzymatic cross-linking: premise of a bioinspired material for food packaging, cosmetics and biomedical applications

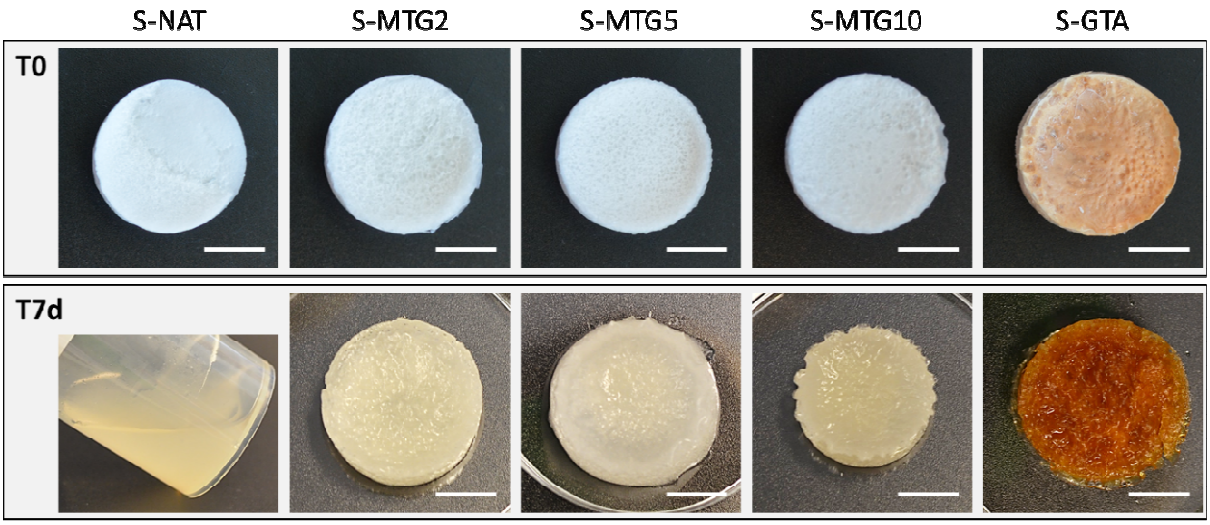

Fig. 11 Macroscopic demonstration of sponge stability after 7 days in hydrated conditions at 40°C (n = 3). S: salmon gelatin, NAT: native gelatin, MTG: enzymatically cross-linked gelatin (the associated number is the % of enzyme), and GTA: chemically cross-linked gelatin. Scale bar: 1 cm.

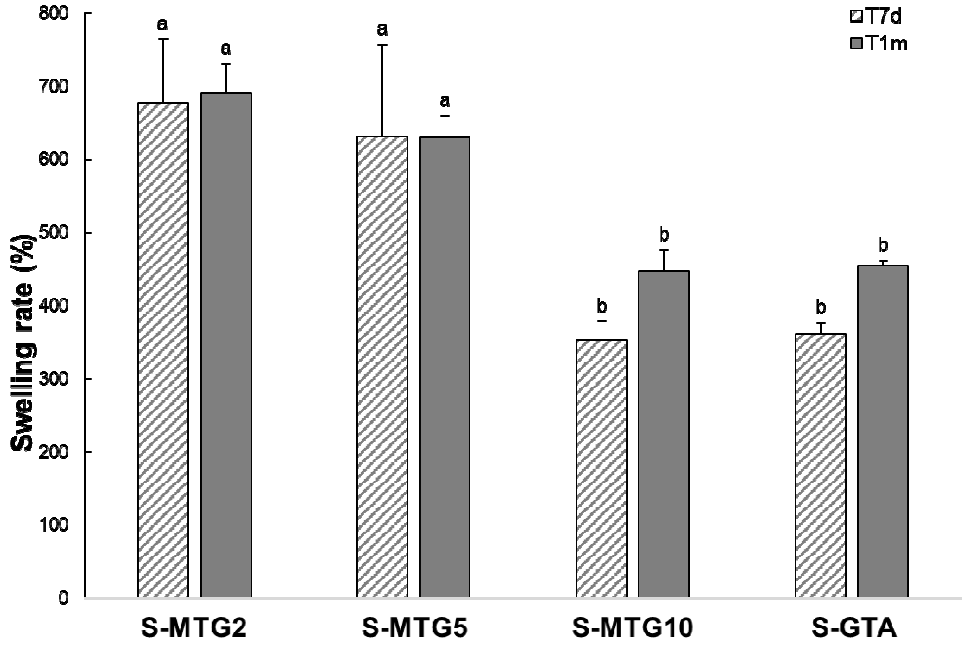

Fig. 12 Swelling rate (%) of cross-linked salmon gelatin sponge after 7 days (T7d - hatched bars) and 1 month (T1m - filled bars) in hydrated conditions at 40°C (n = 3). S: salmon gelatin, MTG: enzymatically cross-linked gelatin (the associated number is the % of enzyme), and GTA: chemically cross-linked gelatin. Different letters above the histogram bars indicate significant differences $P < 0.05$.

Mechanically enhanced *Salmo salar* gelatin by enzymatic cross-linking: premise of a bioinspired material for food packaging, cosmetics and biomedical applications

Table 1 Sample codes and compositions with corresponding gelatin source, microbial transglutaminase (MTG) or glutaraldehyde (GTA) concentrations. S: salmon gelatin, P: porcine gelatin, NAT: untreated sample, MTG: enzymatically cross-linked sample (the associated number is the % of enzyme), and GTA: chemically cross-linked sample.

Sample code	Gelatin % (w/v)	MTG % (w/w protein)	GTA % (v/v)
S-NAT	6.67	-	-
S-MTG2	6.67	2	-
S-MTG5	6.67	5	-
S-MTG10	6.67	10	-
S-GTA	6.67	-	1
P-NAT	6.67	-	-
P-MTG2	6.67	2	-
P-MTG5	6.67	5	-
P-MTG10	6.67	10	-
P-GTA	6.67	-	1

Table 2 Proximate composition of S-NAT.

Analysis	S-NAT
Moisture (%)	7.1 ± 0.4
Fat (%)	1.2 ± 0.5
Protein (%)	93.6 ± 2.8
Ash (%)	1.9 ± 0.2

Table 3 Molecular weight (MW) distribution of the gelatin samples by SEC-HPLC. S-NAT: salmon native gelatin and P-NAT: porcine native gelatin.

MW (kDa)	**Distribution (%)**	
	S-NAT	P-NAT
> 600	41.81	59.84
300-600	26.76	17.23
100-300	20.01	15.03
< 100	11.42	7.90

Table 4 Amino acid composition of native gelatin samples. S-NAT: salmon native gelatin, P-NAT: porcine native gelatin, Pro: proline, and Hyp: hydroxyproline.

Amino acids	**g/100g$_{protein}$**	
	S-NAT	P-NAT
Alanine	8.70 ± 0.70	8.78 ± 0.70
Arginine	7.86 ± 0.63	7.71 ± 0.62
Aspartic acid	6.18 ± 0.49	5.33 ± 0.43
Cystine	0.17 ± 0.03	0.06 ± 0.03
Glutamic acid	9.84 ± 0.79	9.91 ± 0.79
Glycine	23.10 ± 1.85	21.61 ± 1.73
Histidine	1.36 ± 0.11	0.66 ± 0.05
Hydroxylysine	1.17 ± 0.09	1.00 ± 0.08
Hydroxyproline	7.24 ± 0.58	11.3 ± 0.90
Isoleucine	1.17 ± 0.09	1.12 ± 0.09
Leucine	2.24 ± 0.18	2.75 ± 0.22
Lysine	3.22 ± 0.26	3.48 ± 0.28
Methionine	2.18 ± 0.17	0.71 ± 0.06
Phenylalanine	1.89 ± 0.15	1.99 ± 0.16
Proline	11.06 ± 0.88	13.66 ± 1.09
Serine	4.37 ± 0.35	3.22 ± 0.26
Threonine	2.33 ± 0.19	1.65 ± 0.13
Tyrosine	0.47 ± 0.04	0.80 ± 0.06
Valine	1.61 ± 0.13	2.29 ± 0.18
Pro + Hyp	18.3	24.96

Table 5 Average pore cross-sectional size (µm) of salmon gelatin sponges. S: salmon gelatin, NAT: native gelatin, and MTG: enzymatically cross-linked gelatin (the associated number is the % of enzyme). Different letters next to values indicate significant differences $P < 0.05$.

	Mean pore size (µm)
S-NAT	720 ± 287 [a]
S-MTG2	672 ± 277 [a]
S-MTG5	630 ± 196 [a]
S-MTG10	461 ± 233 [b]

Table 6 FTIR relative absorbance of the native and cross-linked samples of salmon gelatin (n = 3). S: salmon gelatin, NAT: native gelatin, MTG: enzymatically cross-linked gelatin (the associated number is the % of enzyme), and GTA: chemically cross-linked gelatin.

	Relative absorbance				
Peaks	S-NAT	S-MTG2	S-MTG5	S-MTG10	S-GTA
Amide I	0.99	0.96	0.97	0.97	0.99
Amide II	0.84	0.81	0.84	0.73	0.67
Amide III	0.49	0.43	0.47	0.31	0.25
Amide A	0.42	0.51	0.36	0.53	0.50
Amide B	0.25	0.29	0.19	0.27	0.24
Ratio amide III / 1450 nm	0.88	0.86	0.78	0.67	0.65